Supporting Information

Graveel et al. 10.1073/pnas.0810403106

SI Methods

***Met* FISH.** Interphase FISH was performed on tumor touch preparations as described previously (1). Hybridization signals were scored for at least 100 nuclei per slide. Metaphase slides were prepared from 24-h primary cultures that were harvested and fixed with methanol/acetic acid (3:1). Slide pretreatment and hybridization were the same as for tumor touch preparations, with exception to aging and digestion which was 2× SSC at 37 °C for 10 min and pepsin treatment for 4 min. FISH probes were prepared from purified BAC clones RP23–73G15 (includes *Met* gene on locus 6A2) and RP24–462C10 (control probe on locus 6D3). Chromosome 6 clones were labeled with SpectrumOrange and SpectrumGreen (Abbott Molecular), respectively, by nick translation. BACs were purchased from the Children's Hospital Oakland Research Institute. Image acquisition was performed with a COOL-1300 SpectraCube camera (Applied Spectral Imaging) mounted on an Olympus BX51 epifluorescence microscope and FISHView software EXPO v5.0 (Applied Spectral Imaging). Hybridization signals were scored for at least 10 metaphases. Cells containing greater than 50 signals were scored as 50 due to the difficulty of counting past that number for interphase FISH.

Spectral Karyotyping. Metaphase spreads were prepared from 24-h primary cultures that were harvested and fixed with methanol/acetic acid (3:1). Five microliters of denatured SkyPaint probe (Applied Spectral Imaging) was added to the metaphase slide, which then was covered with a cover slip and incubated overnight in a 37 °C humidified chamber. Slide preparation and hybridization were performed according to the standard supplied protocol (Applied Spectral Imaging) to investigate cytogenetic abnormalities. Image acquisition was performed with a COOL-1300 SpectraCube camera (Applied Spectral Imaging) mounted on an Olympus BX51 epifluorescence microscope using a spectral karyotyping optical filter (Chroma Technology). For each sample, a minimum of 15 metaphases were analyzed using the HiSKY EXPO v5.0 software (Applied Spectral Imaging).

Immunohistochemical Analysis. To prepare sections, mammary glands and tumors were fixed in 4% phosphate-buffered paraformaldehyde overnight and then transferred to 70% ethanol. Tissues were embedded in paraffin and sectioned at 5 μm. Antigen retrieval and detection were performed using a Discovery XT immunostainer (Ventana Medical Systems). Primary antibodies were revealed with the Ventana DABMap or UltraMap detection kit, and hematoxylin (Ventana Medical Systems) was used as a nuclear counterstain. A negative control reaction with no primary antibody was always performed alongside the reaction-containing sample. Primary antibodies for staining of mouse tissues are as follows: ERα (MC-20; Santa Cruz), ErbB2 (29D8; Cell Signaling), Met (AF527; R&D Systems), and PR (C-19; Santa Cruz). Primary antibodies for staining of human tissues are as follows: Met-4 (2), ER (SP1; LabVision (Neomarkers)), PR (SP2; LabVision (Neomarkers)), Her2 (HER2 rabbit polyclonal; Dako), CK5/6 (D5/16B4; Zymed), and EGFR (31G7; Zymed).

Scoring of Met^{mut} Immunohistochemical Preparations. ER and PR were interpreted as positive based on nuclear staining. Immunohistochemical results were scored based on the percentage of cells showing expression: negative, <5%; positive, ≥5% (3). Intensity of staining was noted but not used for scoring. Her2/ErbB2 expression was evaluated semiquantitatively according to a standard protocol (HercepTest; DakoCytomation). The protocol categorizes tumors into four groups: grade 0, lack of staining in all tumor cells or membrane staining in <10% of the tumor cells; grade 1+, weak, not circumferential membrane staining in >10% of the tumor cells; grade 2+, intermediate, circumferential membrane staining in >10% of the tumor cells; grade 3+, intense and circumferential staining in >10% of the tumor cells.

Immunostaining for Met was scored semiquantitatively on a scale of 0–3: grade 0, lack of staining in all tumor cells or in <10% of the tumor cells; grade 1, weak staining in >10% of the tumor cells; grade 2, intermediate staining in >10% of the tumor cells; and grade 3, intense staining in >10% of the tumor cells. Both cytoplasmic and membrane staining was evaluated in each case. Staining was scored by a pathologist who had no prior knowledge of the clinical data.

Breast Tissue Microarray Construction and Immunohistochemical Subtype Scoring. Human breast tissue microarrays consisting of duplicate 0.6-mm cores (Beecher Instruments) were constructed from archival tumor blocks (formalin-fixed, paraffin-embedded tissue) from 137 patients with invasive breast cancer after surgical intervention at Washington University and Barnes-Jewish Hospital in St. Louis from 1997 to 2003. Human tissue specimens were obtained from the Alvin J. Siteman Cancer Center Tissue Procurement Core facility using an Institutional Review Board-approved protocol. Immunohistochemistry for ER, PR, EGFR, Ck5/6, and Her2 and FISH for Her2 were performed as previously described (4, 5). Her2 score is a dichotomized immunohistochemistry with FISH correction. The dichotomization scheme is as follows: 1, Her2 IHC = (0, 1) = > negative; 2, Her2 IHC = (2) = > positive; 3, Her2 IHC = (2) = > use dichotomized FISH score. The FISH score was dichotomized from the amplification ratio with a cut-off point of 2.0 (i.e., amp ratio < = 2.0 is negative and amp ratio >2.0 is positive). ER and PR scores are dichotomized as <1% nuclei stained vs. ≥1% nuclei stained. EGFR and CK5/6 scores are dichotomized as negative vs. any cytoplasmic and/or membranous staining of malignant cells, above background. Met staining was scored as described for Met^{mut} immunohistochemical sections.

Statistical Analysis. Statistical analysis was performed in SPSS 15.0 for Windows (SPSS). Correlative analysis was done using Fisher's exact test. Univariate analysis of survival was done by calculating Kaplan–Meier survival curves and log-rank statistics. All tests were two-sided and used a 5% alpha level to determine significance. Multiple comparisons were corrected using the Bonferroni–Holmes method (6). Analyses of the duplicate core tissue microarray immunohistochemistry data, where two cores where taken from each specimen and put on the array side by side, was done by taking the higher score between the duplicate cores.

Gene Expression Analysis. All data processing and analysis were performed using BioConductor version 2.0 software (7). Single-color expression profiles derived from breast tumors were previously generated using the HG-133 Plus 2.0 chipset and obtained from the Gene Expression Omnibus (GSE3744). The raw data were preprocessed using the RMA method as implemented in the Affy package using updated probe set mappings

(8, 9). To generate the Met activation signature, gene expression profiling data were generated from wild-type and met-mutant mouse embryonic fibroblasts using two-color in-house pin-printed cDNA microarrays. DNA microarray production, labeling, and hybridization were performed as described (10). Slides were scanned in a commercially available confocal fluorescent Scan Array Lite scanner equipped with lasers operating at 532 and 635 nm (GSI Lumonics). Image files were analyzed by use of GenePix Pro 4 image analysis software (Axon Instruments). The raw data were preprocessed using a pin-tip-dependent normalization method, and differentially expressed genes were identified using linear modeling in which the variance was moderated using an empirical Bayes method as implemented in the limma package (7). Five-hundred fifty-eight genes were identified as being up-regulated in the Met^{M1248T} line, and these genes constituted the *MET* activation signature. This signature was analyzed for enrichment in the breast cancer tumor data using the parametric gene set enrichment analysis approach as implemented in the PGSEA package (11). Standard protocols were followed.

An additional gene expression dataset was used to evaluate if MET expression features were associated with breast cancer patient survival (GSE3165). This dataset was downloaded from the Gene Expression Omnibus, the expression levels of the MET gene were isolated, and a Cox proportional hazards model was used to evaluate MET gene expression with respect to patient outcome. A multifactor model in which MET expression and another clinical/molecular parameter (ER status, basal subtype, etc) was included was used to determine if MET expression was an independent predictor of outcome. To evaluate the MET gene signature with respect to patient outcome, the 558-gene Met gene signature was collapsed to single summary statistics using the PGSEA method. Usually, the enrichment score is calculated with respect to the median expression of the nondiseased samples of the same tissue type. That is before enrichment score calculations; for each gene the median expression level of the nondiseased tissue is subtracted from each tumor expression value. In the GSEA3165 dataset, the enrichment score was calculated relative to the median tumor sample. That is before enrichment score calculations; for each gene the median expression level across the tumor samples was subtracted from each tumor expression value.

1. Graveel C, et al. (2004) Activating Met mutations produce unique tumor profiles in mice with selective duplication of the mutant allele. *Proc Natl Acad Sci USA* 101:17198–17203.
2. Knudsen BS, et al. (2009) A novel multipurpose monoclonal antibody for evaluating human c-Met expression in preclinical and clinical settings. *Appl Immunohistochem Mol Morphol* 17:57–67.
3. Zhang X, et al. (2005) Estrogen receptor positivity in mammary tumors of Wnt-1 transgenic mice is influenced by collaborating oncogenic mutations. *Oncogene* 24:4220–4231.
4. Nielsen TO, et al. (2004) Immunohistochemical and clinical characterization of the basal-like subtype of invasive breast carcinoma. *Clin Cancer Res* 10:5367–5374.
5. Cheang MC, et al. (2008) Basal-like breast cancer defined by five biomarkers has superior prognostic value than triple-negative phenotype. *Clin Cancer Res* 14:1368–1376.
6. Holm S (1979) A simple sequentially rejective multiple test procedure. *Scand J Statist* 6:65–70.
7. Gentleman RC, et al. (2004) Bioconductor: Open software development for computational biology and bioinformatics. *Genome Biol* 5:R80.
8. Irizarry RA, et al. (2003) Exploration, normalization, and summaries of high density oligonucleotide array probe level data. *Biostatistics* 4:249–264.
9. Dai M, et al. (2005) Evolving gene/transcript definitions significantly alter the interpretation of GeneChip data. *Nucleic Acids Res* 33:e175.
10. Takahashi M, et al. (2001) Gene expression profiling of clear cell renal cell carcinoma: gene identification and prognostic classification. *Proc Natl Acad Sci USA* 98:9754–9759.
11. Furge KA, et al. (2007) Identification of deregulated oncogenic pathways in renal cell carcinoma: an integrated oncogenomic approach based on gene expression profiling. *Oncogene* 26:1346–1350.

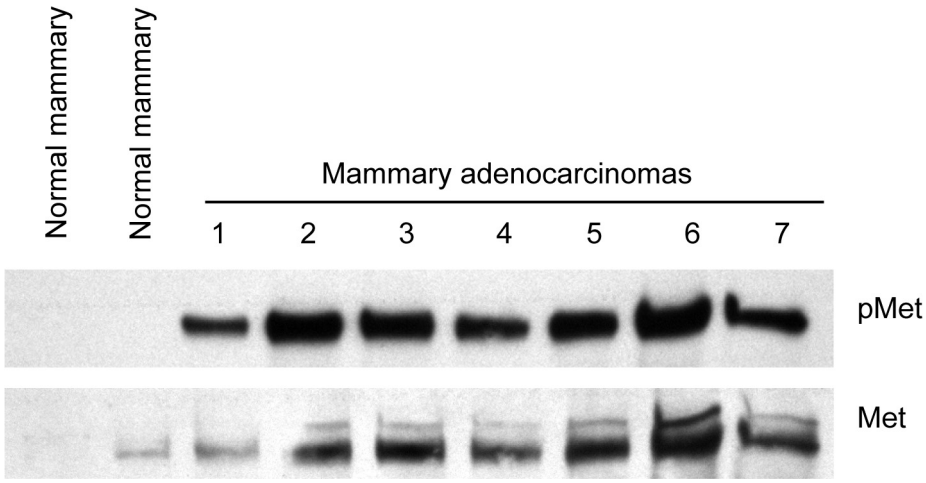

Fig. S1. Met expression is highly up-regulated in Met^{mut} tumors. Expression and activity of Met were determined via immunoprecipitation and Western blot analysis. High levels of Met (p140 and p170) were observed in all tumors, and the processed p140 form of *p*-Met was highly expressed in all tumors. Tumors 1–4 were obtained from multiparous females, and tumors 5–7 were obtained from nulliparous females.

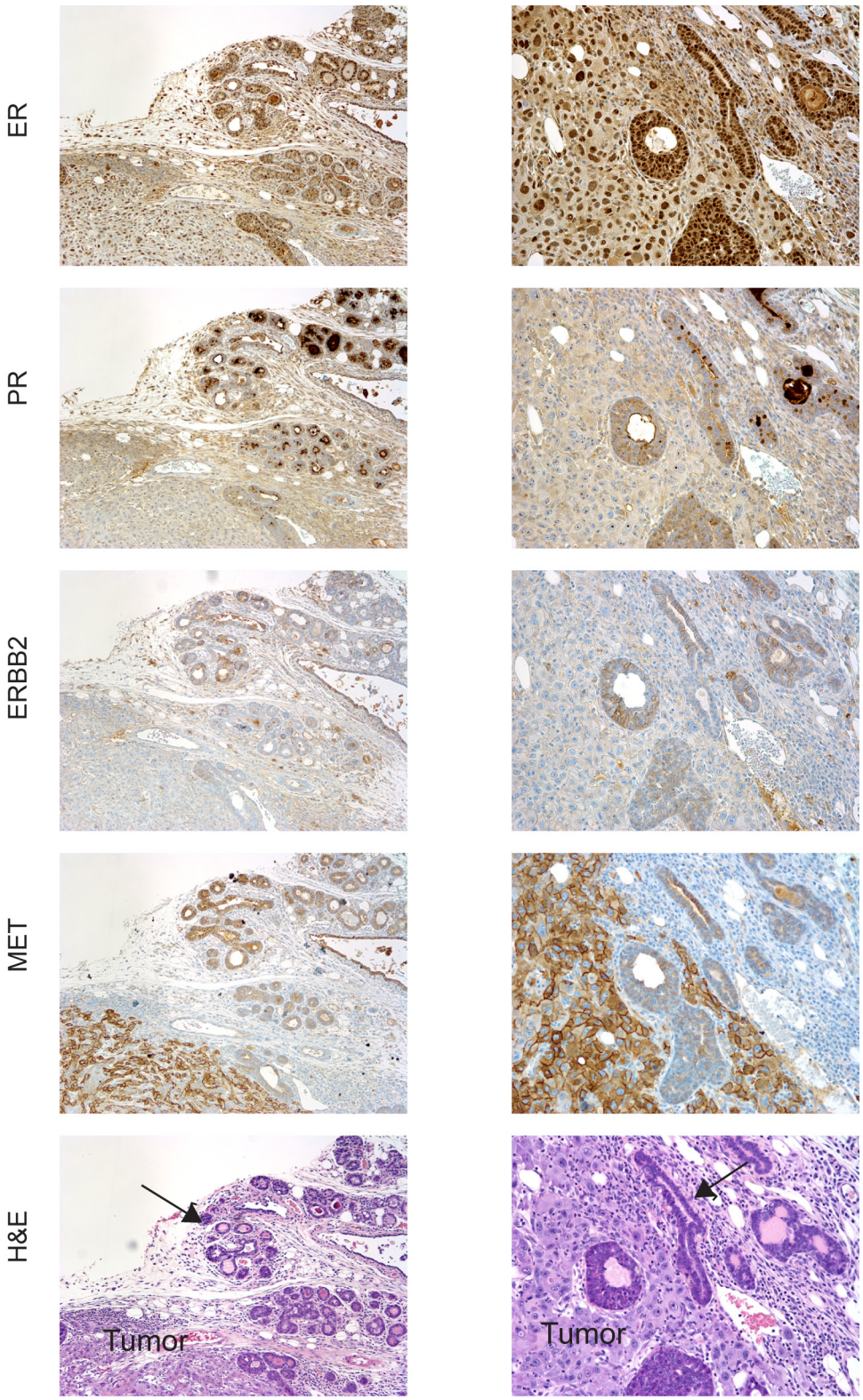

Fig. S2. Met expression is observed in hyperplastic ducts on the outer edge of mammary tumors along with ER, PR, and ErbB2. (*Left*) Staining of hyperplastic ducts (see arrow) at the edge of the mammary tumor (Animal 13; Magnification: 100×). (*Right*) Met staining is stronger in the hyperplastic ducts on the outer edge of the tumor (arrow) compared with the larger duct found within the tumor (Animal 14; Magnification: 200×).

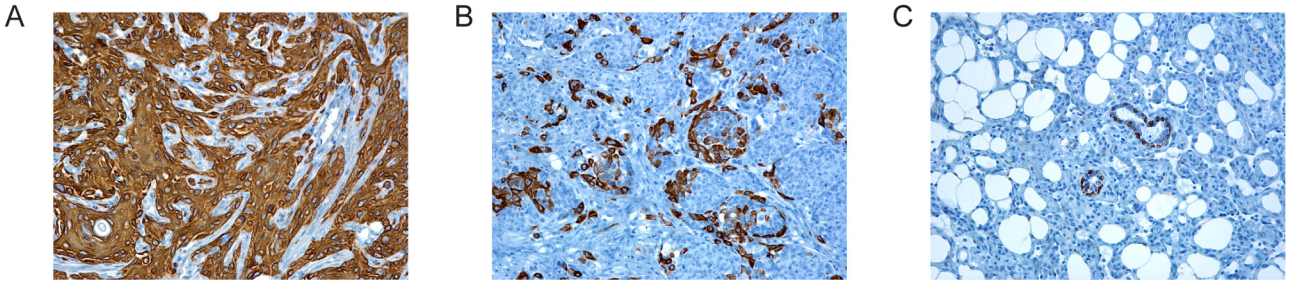

Fig. S3. Cytokeratin 5 (CK5) expression in Met^{mut} tumors. (*A*) CK5 expression in a Met^{mut} squamous cell carcinoma, (*B*) an adenocarcinoma with solid and fibrotic regions, and (*C*) a solid adenocarcinoma. In (*C*), we only observed CK5 staining within normal ducts that were trapped in the tumor. This was the only Met^{mut} tumor in which the whole tumor was classified as solid.

Table S1. Histopathological analysis of Met^{mut} females

Animal no.	Parity	Age (mo)	Mammary pathology	Other tumors
1	Multiparous	8	Adenosquamous carcinoma	
2	Multiparous	8	Myoepithelioma	
3	Multiparous	8	Adenocarcinoma w/ squamous metaplasia	
4	Multiparous	9	Adenocarcinoma w/ squamous metaplasia	
5	Multiparous	9	Adenocarcinoma w/ squamous metaplasia	
6	Multiparous	10	Squamous cell carcinoma	
7	Multiparous	9	Adenosquamous carcinoma	
8	Multiparous	11	No tumor	
9	Multiparous	8	Adenosquamous carcinoma	
10	Multiparous	12	Adenocarcinoma w/ squamous metaplasia	
11	Multiparous	12	No tumor	
12	Multiparous	14	Adenocarcinoma w/ squamous metaplasia Adenocarcinoma w/ solid patterns	Undifferentiated sarcoma
13	Multiparous	12	Adenosquamous carcinoma Adenocarcinoma w/ solid patterns	
14	Multiparous	13	Adenocarcinoma w/ squamous metaplasia Adenocarcinoma w/ solid patterns	
15	Multiparous	13	Adenocarcinoma w/ solid patterns	
16	Nulliparous	18	Adenocarcinoma w/ squamous metaplasia and solid patterns	Hemangiosarcoma
17	Nulliparous	9	Adenocarcinoma w/ squamous metaplasia	Hemangioma
18	Nulliparous	5	No tumor	
19	Nulliparous	5	No tumor	
20	Nulliparous	8	Adenocarcinoma w/ squamous metaplasia	
21	Nulliparous	9	No tumor	
22	Nulliparous	5	No tumor	Hemangiosarcoma
23	Nulliparous	13	Adenocarcinoma w/ squamous metaplasia	
24	Nulliparous	13	Myoepithelioma	Hemangiosarcoma
25	Nulliparous	13	Adenocarcinoma	Rhabdomyosarcoma
26	Nulliparous	14	Adenocarcinoma w/ solid patterns Adenocarcinoma w/ squamous metaplasia	Bronchial adenocarcinoma
27	Nulliparous	15	No tumor	Hemangioma
28	Nulliparous	15	Adenosquamous carcinoma w/ solid patterns	
29	Nulliparous	14	Myoepithelioma	
30	Nulliparous	16	Adenocarcinoma w/ solid patterns	
31	Nulliparous	14	No tumor	

The pathology of 31 females was evaluated, and the mammary tumors presented with diverse histological phenotypes including squamous metaplasia, myoepitheliomas, and solid patterns. Several animals developed other tumors, which are described in the right column. No obvious difference in pathology was observed between multiparous and nulliparous females. Squamous metaplasia was determined significant if present in >25% of the tumor. Tumors were defined as adenosquamous or squamous cell carcinoma if metaplasia was present in >50% and >75%, respectively. Squamous metaplasia was observed in 63% of tumors, and solid patterns were present in 30% of tumors.

Table S2. Interphase FISH analysis of Met^{mut} mammary tumors

Animal no.	Met	Control
1	2–50	2–11
5	2–50	2–13
6	2–50	2–8
7	2–50	2–10
16	2–50	2–8
17	2–50	2–8

Relative copy number of *Met* was measured using dual-color interphase FISH on tumor touch preparations. For each tumor, at least 100 nuclei were analyzed. Nuclei in which 50 *Met* signals were observed were too difficult to numerate and are listed as 50; more than 50 copies of Met are likely to be present. FISH analysis was also performed on normal mammary tissue from three Met^{mut} and Met^{WT} animals (data not shown). There were no significant amplifications observed or differences between the Met^{mut} and Met^{WT} animals.

Table S3. Metaphase FISH and spectral karyotyping analysis of Met^{mut} mammary tumors

Animal no.	Analysis
	Metaphase FISH analysis
25	41~42.ish 6D3(RP24–462C10 × 2),6A1(Met x 16~36)[6] 82~85.ish 6D3(RP24–462C10 × 4),6A1(Met x 19~62)[4]
29	39~43.ish 6D3(RP24–462C10 × 2),6A1(Met x 22~84)[10]
30	39~42.ish 6D3(RP24–462C10 × 2),6A1(Met x 2)[9] (normal) 40~41.ish 6D3(RP24–462C10 × 3),6A1(Met x 3)[9] (trisomy 6) 41~42.ish 6D3(RP24–462C10 × 2),6A1(Met x 6~54)[8] 83.ish 6D3(RP24–462C10 × 4),6A1(Met x > 110)[1]
	Composite karyotype for spectral karyotyping analysis
25	41~42 < 2n>,XX,+1[8],+15[12][cp13]/81~84 < 4n>,XXXX,+1x2[1],+15x2[2][cp2]
29	41~42 < 2n>,XX,+1[3],+2[19],+13[2],+15[27][cp27]/82 < 4n>,XXXX,+15x2[cp1]
30	40~42 < 2n>,XX,+1[8],+3[2],+6[3],+15[8][cp14]/81~84 < 4n>,XXXX,+1x2[2],+6[1],+15x2[2][cp3]

For metaphase FISH analysis, at least 10 metaphase spreads were analyzed for each tumor. Most tumors had diploid and tetraploid cell populations, and all tumors showed extrachromosomal *Met* amplification in the form of double minutes. Spectral karyotyping analysis also confirmed diploid and tetraploid cells for each tumor, along with revealing trisomy of chromosomes 1, 2, and 15. A low occurrence of trisomy of chromosomes 3, 6, and 13 was also found in some tumors. A minimum of 15 metaphases were analyzed for spectral karyotyping.

Table S4. Met^{mut} tumors are ER^{+}/PR^{-} with variable ERBB2 expression

Animal No.	ER	PR	ErbB2	Pathology
6a	+	−	−	Squamous cell carcinoma
6b	+	−	+	Hyperplastic nodule
13a	+	−	−	Adenosquamous carcinoma
13b	+	−	+	Adenocarcinoma w/ solid patterns
14a	+	−	−	Adenocarcinoma w/ solid patterns
14b	+/−	−	+	Adenocarcinoma w/ squamous metaplasia
16	+	−	−	Adenocarcinoma w/ squamous metaplasia
17	+	−	−	Adenocarcinoma w/ squamous metaplasia
28	+	−	+	Adenosquamous carcinoma w/ solid and tubular patterns
29	+	−	−	Myoepithelioma
Normal	+	+	+	Normal gland
Normal	+	+	+	Normal gland

ER, PR, and ERBB2 status was determined by immunohistochemistry staining. ER and PR were considered positive if >5% of tumor cells had nuclear staining. ERBB2 status was determined by Hercept scoring (see *SI Methods*). Ninety-two percent of tumors were ER^{+}, and 100% were PR^{-}. Significant but weak ERBB2 staining was observed in 50% of tumors. All tumors had strong MET expression.

Table S5. Description of human breast cancer tissue microarray

Core ID	Grade	Size	Distant metastasis	Node status	CK5/6	EGFR	ER	ERBB2	PR	Subtype
1	3	3	0	2	0	0	0	0	0	Basal TNP
2	3	2	0	1	0	0	0	0	0	Basal TNP
3	3	4	0	1	1	0	0	0	0	Basal
4	2	4	1	1	0	0	0	0	0	Basal TNP
5	3	2	0	1	ND	ND	ND	ND	ND	Unassignable
6	2	1	0	0	0	0	1	0	1	Luminal A
7	3	4	0	1	ND	ND	ND	0	ND	Unassignable
8	3	3	0	1	1	1	0	0	0	Basal
9	3	3	0	0	0	1	0	ND	0	Unassignable
10	3	3	0	0	1	1	0	0	1	Luminal A
11	3	4	0	1	0	1	0	1	0	Her2
12	3	2	0	1	ND	ND	0	ND	ND	Unassignable
13	3	2	1	0	0	0	0	−4	0	Unassignable
14	3	2	0	1	ND	ND	ND	ND	ND	Unassignable
15	2	2	0	1	0	ND	1	ND	1	Unassignable
16	3	2	0	1	0	0	0	0	0	Basal TNP
17	2	2	0	1	0	0	0	0	0	Basal TNP
18	3	2	0	1	ND	ND	ND	ND	ND	Unassignable
19	2	1	0	1	0	0	1	0	1	Luminal A
20	2	1	0	0	0	0	1	0	1	Luminal A
21	2	3	0	1	0	0	1	0	1	Luminal A
22	2	2	0	1	0	0	1	0	1	Luminal A
23	3	2	0	0	1	0	0	0	0	Basal
24	3	2	0	1	0	0	1	0	1	Luminal A
25	3	1	0	0	0	1	0	0	0	Basal
26	2	1	0	0	0	0	1	0	1	Luminal A
27	2	1	0	0	0	0	1	0	0	Luminal A
28	3	ND	ND	ND	0	0	1	0	0	Luminal A
29	1	2	0	0	0	0	1	ND	1	Unassignable
30	3	2	0	1	0	0	0	0	0	Basal TNP
31	3	2	0	0	1	0	0	0	0	Basal
32	2	4	0	1	0	0	1	0	1	Luminal A
33	3	3	0	1	1	1	0	0	0	Basal
34	3	2	0	1	0	0	1	0	1	Luminal A
35	3	2	0	1	0	0	1	ND	1	Unassignable
36	2	1	0	0	0	0	1	ND	1	Unassignable
37	3	2	0	0	1	0	0	0	0	Basal
38	2	1	1	1	0	0	1	0	1	Luminal A
39	3	2	0	1	0	0	1	0	1	Luminal A
40	3	3	0	1	0	0	0	0	0	Basal TNP
41	2	2	0	1	ND	ND	ND	0	ND	Unassignable
42	3	1	0	0	0	0	1	0	0	Luminal A
43	3	2	0	1	0	0	1	0	0	Luminal A
44	3	2	0	0	0	0	0	0	0	Basal TNP
45	3	2	0	1	0	0	1	0	1	Luminal A
46	3	4	0	1	0	0	1	0	1	Luminal A
47	2	2	0	1	0	0	1	0	1	Luminal A
48	ND	1	0	0	0	0	1	0	1	Luminal A
49	2	4	0	1	0	0	1	0	1	Luminal A
50	3	2	0	0	1	1	0	0	0	Basal
51	3	2	0	0	1	0	0	0	0	Basal
52	2	1	0	1	ND	0	1	0	1	Luminal A
53	3	2	0	0	1	1	0	0	0	Basal
54	3	2	0	0	0	0	1	0	0	Luminal A
55	1	1	0	0	ND	ND	ND	ND	ND	Unassignable
56	1	2	0	0	0	0	1	0	0	Luminal A
57	1	2	0	0	0	0	1	0	1	Luminal A
58	3	1	0	0	0	0	1	0	1	Luminal A
59	3	3	0	0	0	0	0	0	0	Basal TNP
60	3	2	0	1	0	0	0	0	0	Basal TNP
61	3	2	0	0	1	1	0	0	0	Basal
62	3	2	0	0	0	0	1	0	0	Luminal A
63	3	2	0	1	0	0	1	0	0	Luminal A
64	3	2	0	1	0	0	1	0	1	Luminal A

Core ID	Grade	Size	Distant metastasis	Node status	CK5/6	EGFR	ER	ERBB2	PR	Subtype
65	2	2	0	1	0	0	1	1	1	Luminal B
66	3	1	0	1	0	0	0	0	0	Basal TNP
67	ND	ND	ND	ND	ND	ND	ND	ND	ND	Unassignable
68	2	1	0	1	ND	ND	ND	ND	ND	Unassignable
69	3	2	0	1	0	0	1	0	1	Luminal A
70	2	4	0	0	0	0	1	0	1	Luminal A
71		2	0	1	0	0	1	0	0	Luminal A
72	3	2	0	1	1	1	0	ND	0	Unassignable
73	3	1	0	1	0	0	0	0	0	Basal TNP
74	3	2	0	0	0	0	0	0	1	Luminal A
75	3	2	0	1	1	1	0	0	0	Basal
76	3	2	0	1	0	0	0	1	0	Her2
77	3	1	0	0	0	0	0	0	0	Basal TNP
78	3	1	0	0	0	0	1	0	0	Luminal A
79	2	3	0	0	0	1	0	0	0	Basal
80	3	2	0	0	0	1	0	0	0	Basal
81	3	2	0	0	ND	0	1	0	1	Luminal A
82	3	4	0	1	0	0	0	0	0	Basal TNP
83	3	1	0	1	0	0	0	1	0	Her2
84	3	2	0	0	0	0	1	0	0	Luminal A
85	3	2	0	0	0	0	0	0	0	Basal TNP
86	3	4	0	1	0	0	0	1	0	Her2
87	3	2	0	1	0	0	0	0	0	Basal TNP
88	3	2	0	0	0	0	0	1	0	Her2
89	3	2	0	0	ND	ND	ND	ND	ND	Unassignable
90	2	1	0	0	0	1	0	0	0	Basal
91	3	2	0	0	1	1	0	0	0	Basal
92	3	2	0	1	0	0	0	0	0	Basal TNP
93	3	3	0	0	0	0	1	0	0	Luminal A
94	3	1	0	1	0	0	0	0	0	Basal TNP
95	3	1	0	0	1	0	0	1	0	Her2
96	1	1	0	1	0	0	0	0	1	Luminal A
97	3	4	0	1	0	1	0	0	0	Basal
98	3	2	0	0	0	0	0	0	0	Basal TNP
99	3	2	0	0	0	0	0	0	0	Basal TNP
100	3	2	0	1	0	1	0	0	0	Basal
101	3	3	0	0	0	0	1	0	0	Luminal A
102	3	1	0	0	0	1	0	0	0	Basal
103	3	2	0	0	0	0	1	1	0	Luminal B
104	3	3	0	1	1	ND	0	ND	0	Unassignable
105	3	2	0	0	0	1	0	0	0	Basal
106	3	1	0	0	1	ND	0	ND	0	Unassignable
107	3	1	0	0	0	0	1	0	1	Luminal A
108	2	1	0	0	0	0	1	0	0	Luminal A
109	3	2	0	0	0	0	0	0	0	Basal TNP
110	3	1	0	1	0	0	1	1	0	Luminal B
111	3	2	0	1	ND	ND	ND	ND	ND	Unassignable
112	3	1	0	1	0	0	0	1	0	Her2
113	2	1	0	0	0	0	0	0	1	Luminal A
114	3	2	0	1	0	0	0	1	0	Her2
115	3	2	0	1	1	0	1	0	1	Luminal A
116	2	2	0	1	0	0	1	0	1	Luminal A
117	3	1	0	0	0	1	0	0	0	Basal
118	2	1	0	1	0	0	1	0	1	Luminal A
119	2	3	0	1	0	0	1	0	1	Luminal A
120	2	1	0	0	0	0	1	0	1	Luminal A
121	3	2	0	1	0	1	0	ND	0	Unassignable
122	3	3	0	1	0	0	1	0	0	Luminal A
123	3	2	0	1	ND	ND	1	0	0	Luminal A
124	2	1	0	0	1	1	0	0	0	Basal
125	2	3	0	1	1	0	0	1	0	Her2
126	3	2	0	1	0	0	1	ND	1	Unassignable
127	1	2	0	0	0	0	0	1	0	Her2
128	3	2	0	0	0	0	1	0	1	Luminal A
129	3	2	0	1	0	0	1	0	0	Luminal A

Core ID	Grade	Size	Distant metastasis	Node status	CK5/6	EGFR	ER	ERBB2	PR	Subtype
130	3	1	0	0	0	0	1	0	0	Luminal A
131	3	1	0	1	ND	ND	ND	0	ND	Unassignable
132	2	1	0	0	ND	0	1	0	0	Luminal A
133	3	2	0	0	0	0	1	0	0	Luminal A
134	2	2	0	1	0	0	1	0	1	Luminal A
135	2	1	0	0	1	1	0	0	0	Basal
136	3	1	0	0	1	ND	0	ND	0	Unassignable
137	Spleen									
138	Spleen									
139	3	2	0	0	ND	ND	ND	ND	ND	Unassignable
140	3	1	0	0	ND	ND	ND	ND	ND	Unassignable
141	3	1	0	1						
142	spleen									
143	spleen									

Human breast tissue microarrays were constructed from archival tumor blocks from 137 patients with invasive breast cancer. Immunohistochemistry for ER, PR, EGFR, CK5/6, and ERBB2 and FISH for ERBB2 was performed as previously described (4, 5). Tumor size (1, ≤2 cm; 2, >2 cm to ≤5 cm; 3, >5 cm; 4, any size with direct extension to chest wall or skin); status of distant metastasis (0, none; 1, yes), node status (0, no positive nodes, 1, 1 or more positive nodes), immunohistochemical scoring, and molecular subtype are shown for each core. Subtype definitions were as follows: luminal A (ER^+ and/or PR^+, $ERBB2^-$), luminal B (ER^+ and/or PR^+, $ERBB2^+$), basal (ER^-, PR^-, $ERBB2^-$, CK 5/6 positive, and/or $EGFR^+$), basal TNP (ER^-, PR^-, $ERBB2^-$); $ERBB2^+$ (ER^-, PR^-, and $ERBB2^+$), and unassignable. ND = not determined.

Table S6. MET expression correlates with ER$^-$, ER$^-$/ERBB2$^-$, and basal cancers

	Spearman correlation	*P* value	*P* value after correction for multiple comparison
MET (≥3) vs. ER	−0.259	0.004	0.016
MET (≥3) vs. ER/ERBB2	−0.239	0.012	0.024
MET (≥3) vs. basal/luminal subtype	0.311	0.005	0.015

Met expression equal to 3 correlated with ER$^-$ and ER$^-$/ERBB2$^-$ cancers and the basal subtype as represented in Fig. 5.